2014 Spring

“Advanced Physical Metallurgy”

- Bulk Metallic Glasses -

05.22.2014

Eun Soo Park

Office: 33-313
Telephone: 880-7221
Email: espark@snu.ac.kr
Office hours: by appointment

• Amorphous vs Nanocrystalline

1) Microstructural observation

XRD, (HR)TEM, EXAFS …

2) Thermal analysis

DSC (Differential Scanning Calorimetry)

: Measure heat absorbed or liberated during heating or cooling

cf) - glass → nucleation & growth

(perfect random)

- ***local clustering*: quenched-in nuclei → *only growth***
- ***Nanocrystalline → growth***

→ local clusters with atomic scale are difficult to identify by conventional observation tools of microstructure.

: Characterization of structure by pair distribution function

3) Intensive Structural Analysis*: *radial distribution function

THERMODYNAMICS OF CRYSTALLIZATION

Crystallization Behaviors in Metallic Glass

Metallic glasses crystallize by a nucleation and growth process.

The driving force is the free energy difference between the glass and the appropriate crystalline phase. → (Free energy vs. Composition diagram)

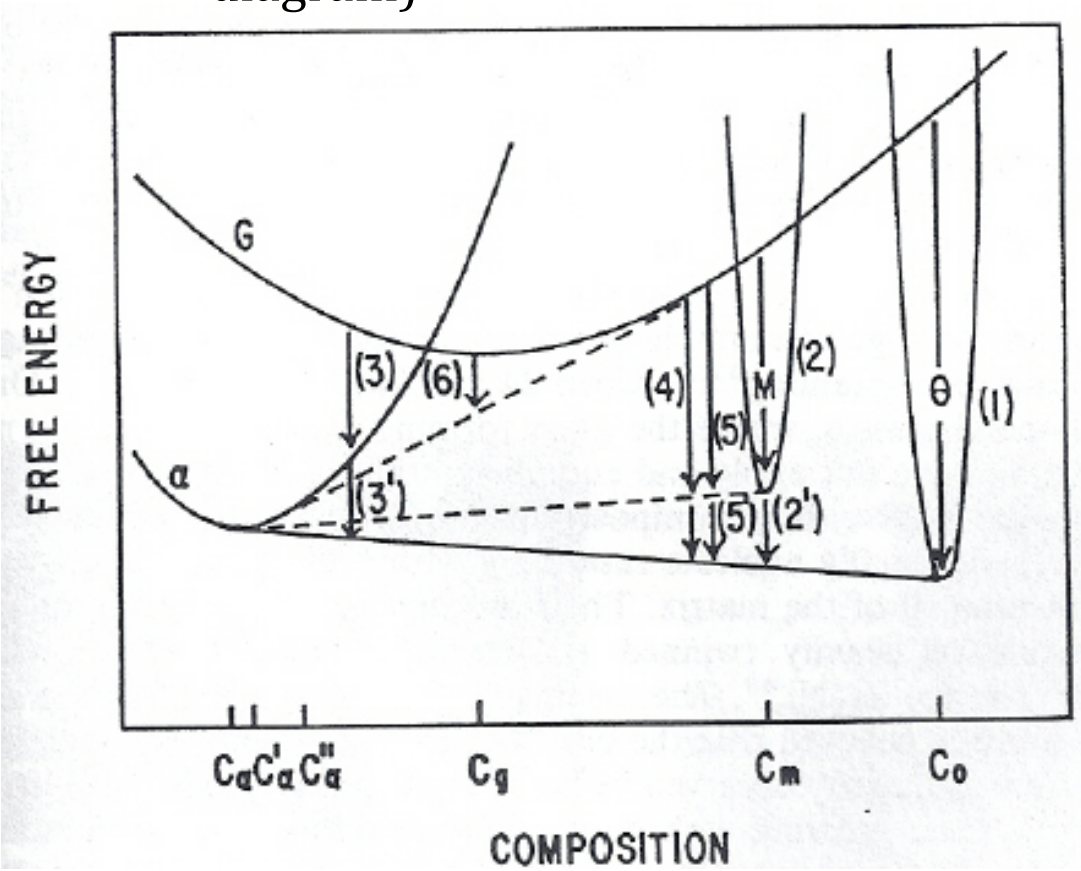

Crystallization mechanisms

1. **Polymorphous Crystallization** of the glass to a crystalline phase of the same composition.
2. **Eutectic Crystallization**
3. **Primary Crystallization** of supersaturated solid solution

G: Glass

α : Solid solution (Crystalline phase)

θ : Intermetallic phase

M: metastable phase

Variation of T_g depending on alloy compositions → Broken Bonds

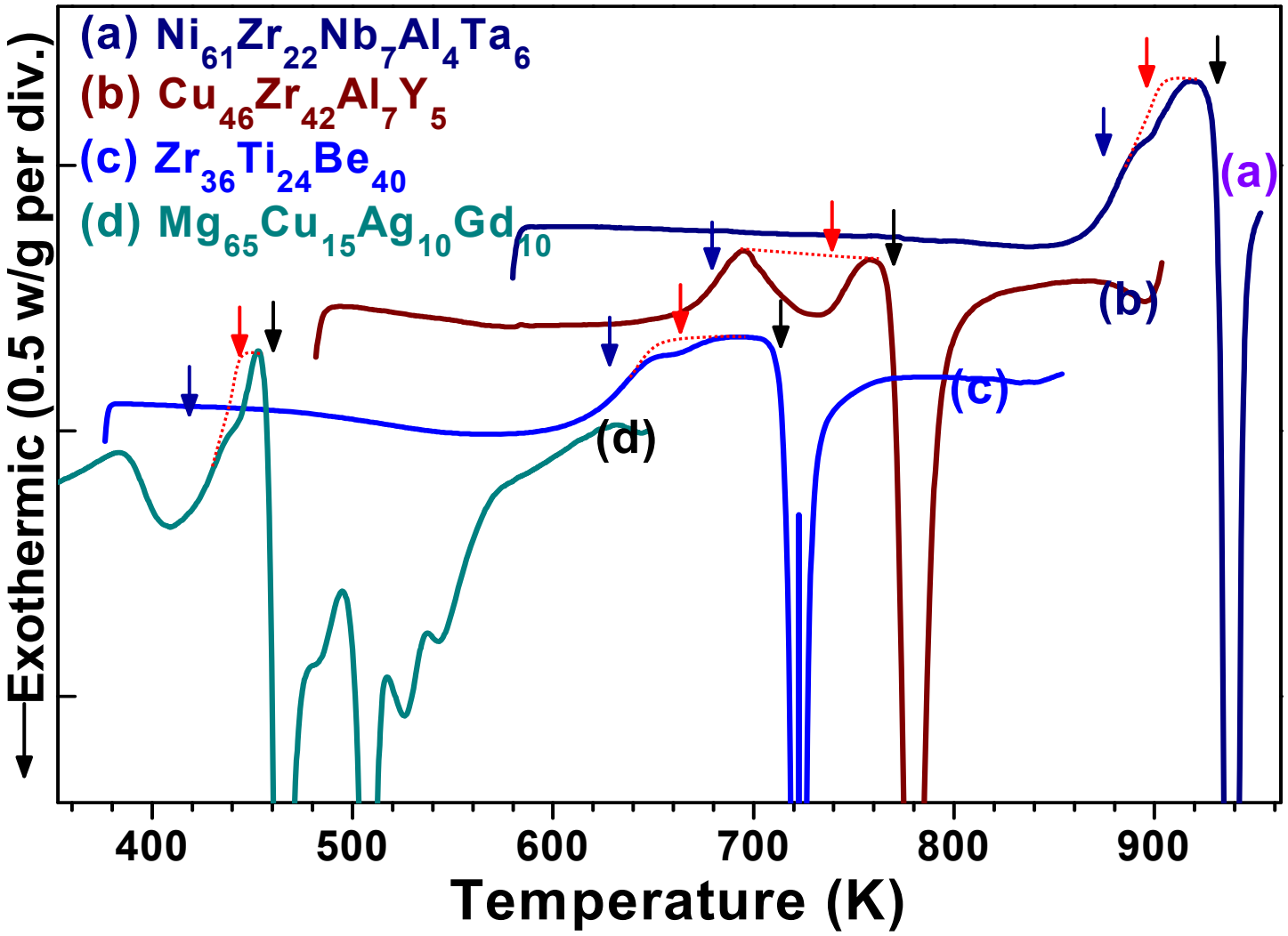

5.5. Thermal Stability of Metallic Glasses

(a) Variation of T_g and T_x in the $Zr_{65}Al_xCu_{35-x}$ (x=0, 7.5, 20) alloys

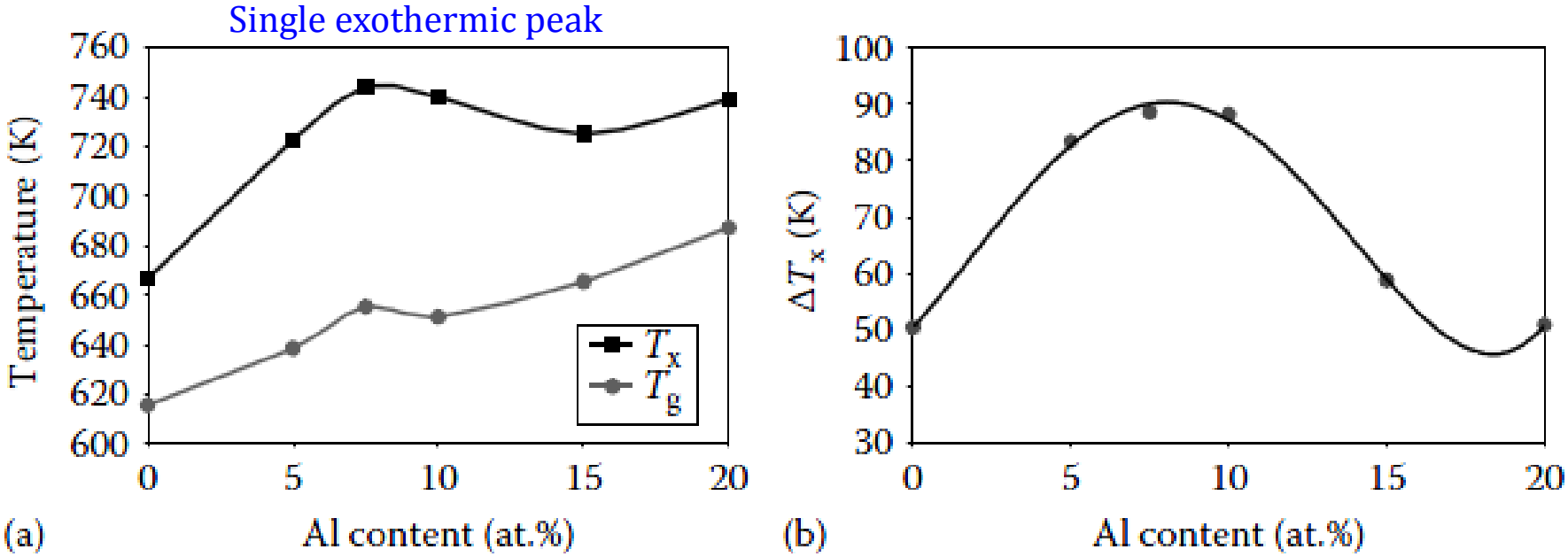

FIGURE 5.7
Variation of (a) T_g and T_x temperatures, and (b) the width of the supercooled liquid region ΔT_x (= $T_x - T_g$), with Al content in the $Zr_{65}Al_xCu_{35-x}$ glassy alloys. (Reprinted from Inoue, A. et al., *Mater. Sci. Eng. A*, 178, 255, 1994. With permission.)

5.6. Crystallization Temperatures and Their Compositional Dependence

Compositional dependence.

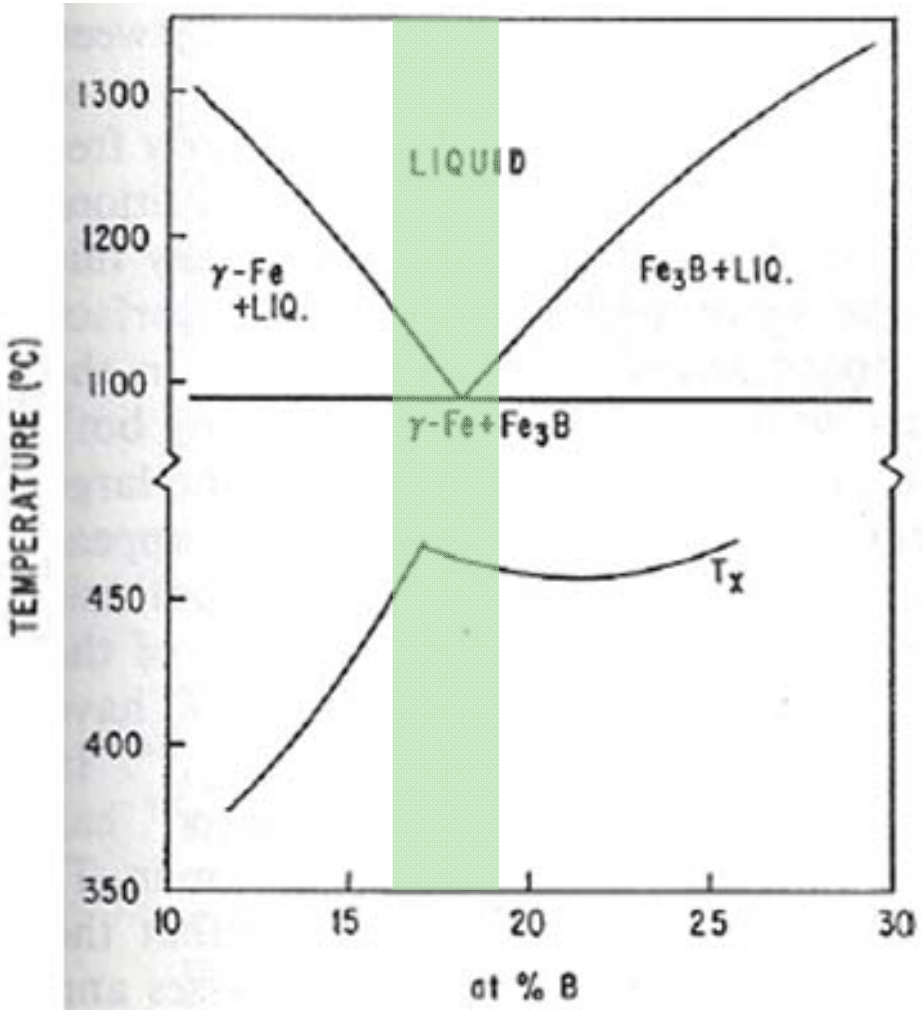

In many binary

Metal-Metalloid glass (Fe-B)

Tx is a maximum near the eutectic composition

The same does not appear to be the

case in all-metal glasses

Metal-Metal glass (Ni-Zr)

A monotonic decrease of Tx with increasing Zr content despite the existence in two eutectics

5.6. Crystallization Temperatures and Their Compositional Dependence

Compositional dependence.

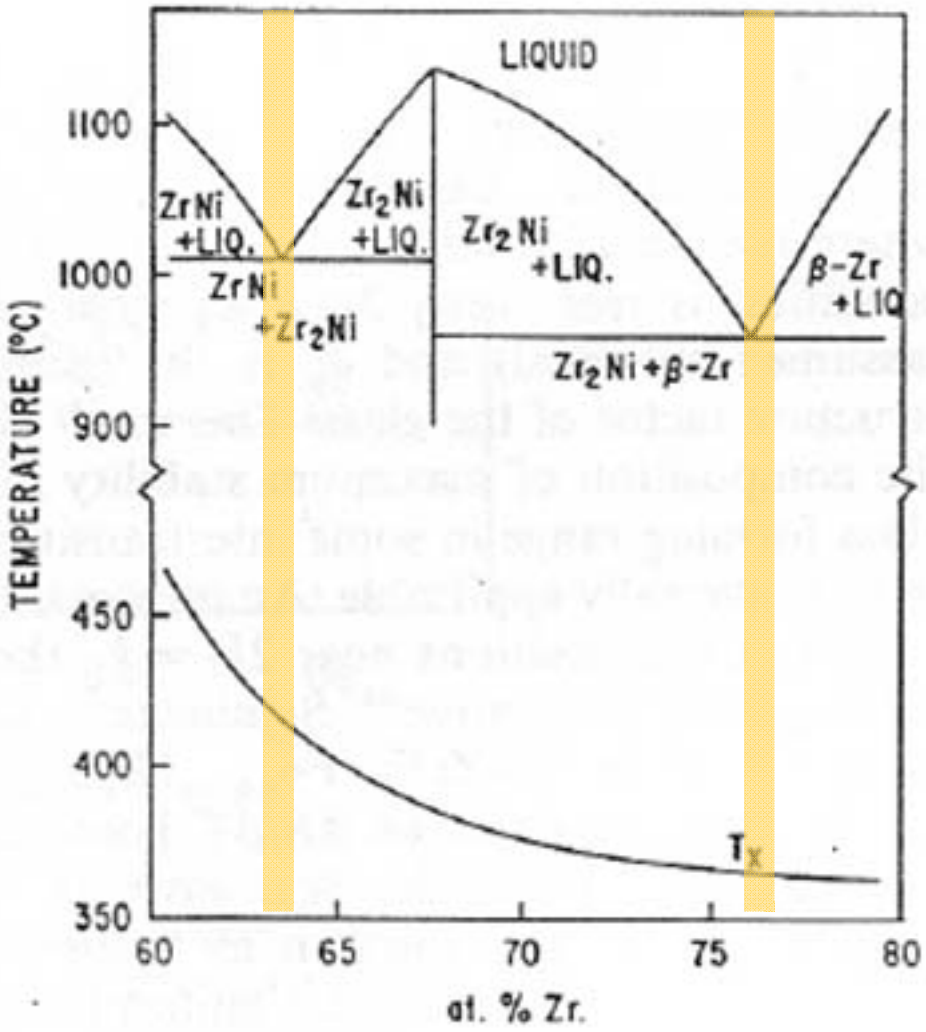

In many binary

Metal-Metalloid glass (Fe-B)

Tx is a maximum near the eutectic composition

The same does not appear to be the

case in all-metal glasses

Metal-Metal glass (Ni-Zr)

A monotonic decrease of Tx with increasing Zr content despite the existence in two eutectics

5.5. Thermal Stability of Metallic Glasses

(b) Arrhenius plot of the incubation time for the precipitation of crystalline phases (τ) in the $Zr_{65}Al_xCu_{35-x}$ (x=0, 7.5, 20) alloys

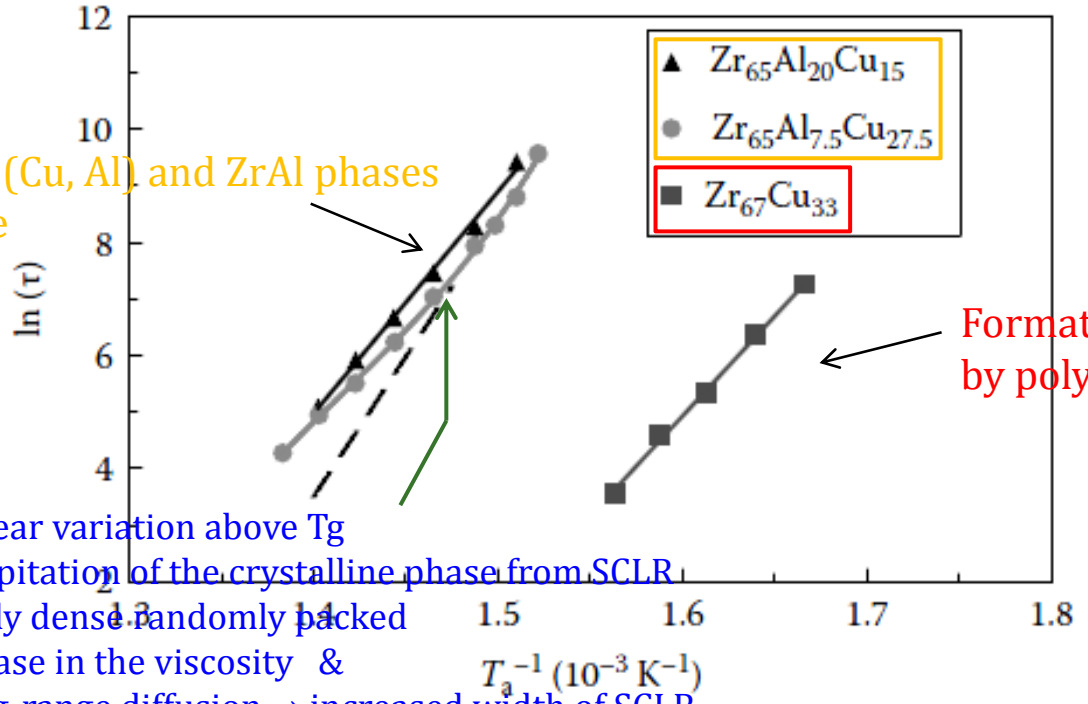

$$\tau \propto \frac{T\eta}{(T_\ell - T)^2}$$

Formation of $Zr_2(Cu, Al)$ and ZrAl phases by eutectic mode

Formation of Zr_2Cu phase by polymorphous mode

Shifted from the linear variation above Tg → suppressed precipitation of the crystalline phase from SCLR due to possess highly dense randomly packed structures → increase in the viscosity & difficult to have long-range diffusion → increased width of SCLR

FIGURE 5.8
Arrhenius plot of the incubation time, τ for the precipitation of crystalline phases in the binary $Zr_{67}Cu_{33}$, and ternary $Zr_{65}Al_{7.5}Cu_{27.5}$ and $Zr_{65}Al_{20}Cu_{15}$ alloys. Note the deviation of τ to the positive side of the linear variation (to higher temperatures) only for the ternary $Zr_{65}Al_{7.5}Cu_{27.5}$ alloy, signifying the delayed crystallization in the alloy with 7.5 at.% Al. Such a deviation is not observed for the other alloys. (Reprinted from Inoue, A. et al., *Mater. Sci. Eng. A*, 178, 255, 1994. With permission.)

(C) Annealing up to T_a at a heating rate of 0.17 K/s (10K/min), annealed there for 60s
→ measure peak temperatures for the nucleation and growth reactions of the crystalline phases in the $Zr_{65}Al_xCu_{35-x}$ (x=0, 7.5) alloys

* Difference in the reciprocals of the Tp between the Pre-annealed and as-quenched samples

688 K, correspond to the peak temp. of the nucleation event of a crystalline phase formation

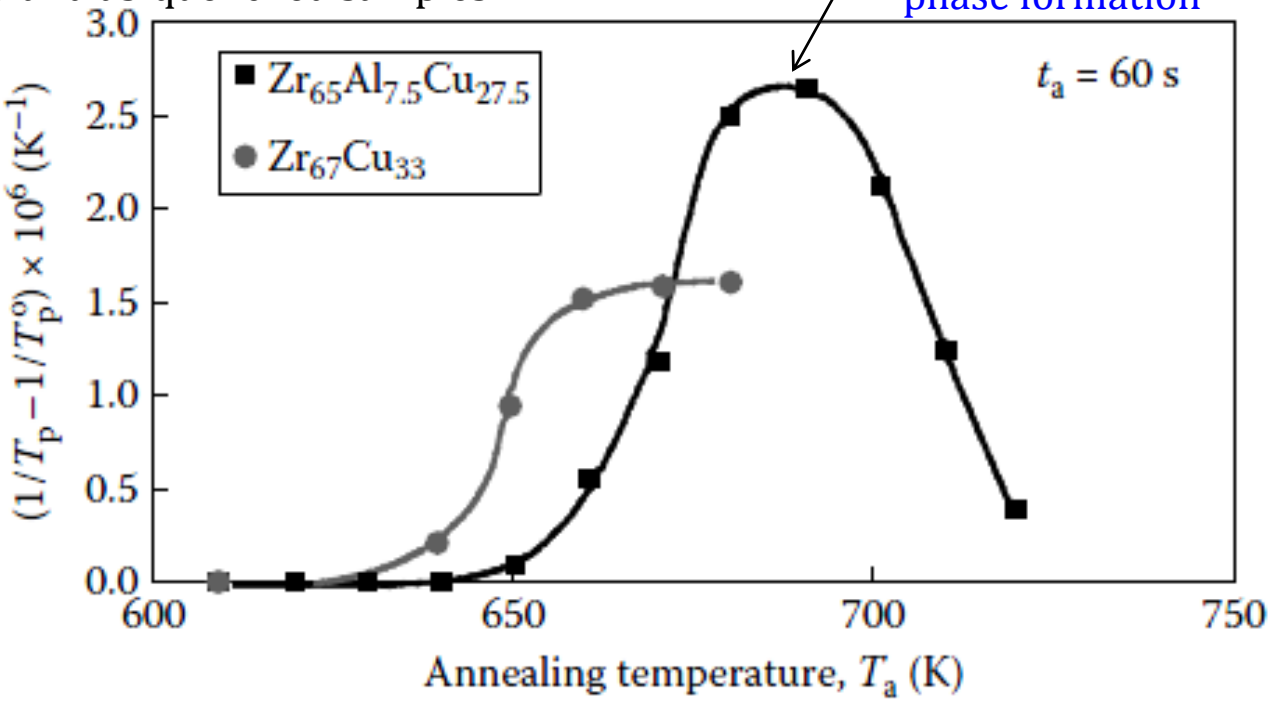

* Measure Tx at a very high heating rate of 5.33 K/s (320 K/min) = corresponding to the maximum growth rates, that is growth temperature
- Zr67Cu33: Just above the maximum temp of 670 K/ difference ~ very small
- Zr65Al7.5Cu27.5: the difference btw max nucleation and max growth temp. ~143K, resulting in enhanced resistance to crystallization (high thermal stability)

* Heating rate ↑ – not significantly increase the grain size in Zr67Cu33 ↔ considerably large grain size in Zr65Al7.5Cu27.5 due to the presence of fewer nuclei

5.7. Annealing of Bulk Metallic Glasses: SR → SCLR (& PS) → Crystallization

Figure 5.11 Different pathways for a metallic glass to crystallize into the equilibrium phases

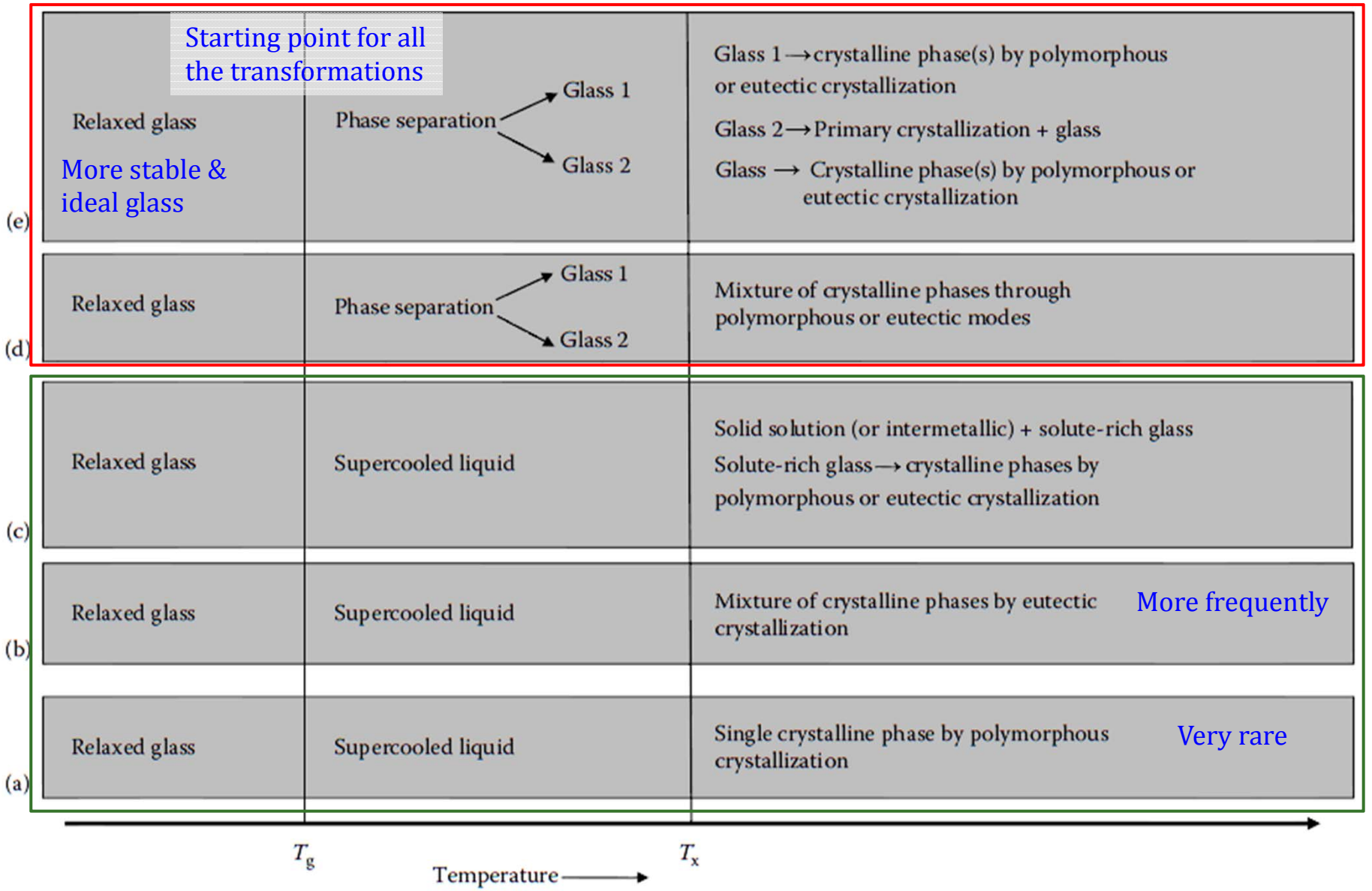

5.7. Annealing of Bulk Metallic Glasses: SR → SCLR (& PS) → Crystallization

5.7.1 Structural Relaxation

RELAXATION BEHAVIOR

Structural relaxation = stabilization

On annealing, the as-synthesized glass slowly transforms toward an "ideal" glass of lower energy through structural relaxation. = annihilation of "defects" or free volume, or recombination of the defects of opposing character, or by changes in both topological and compositional SRO

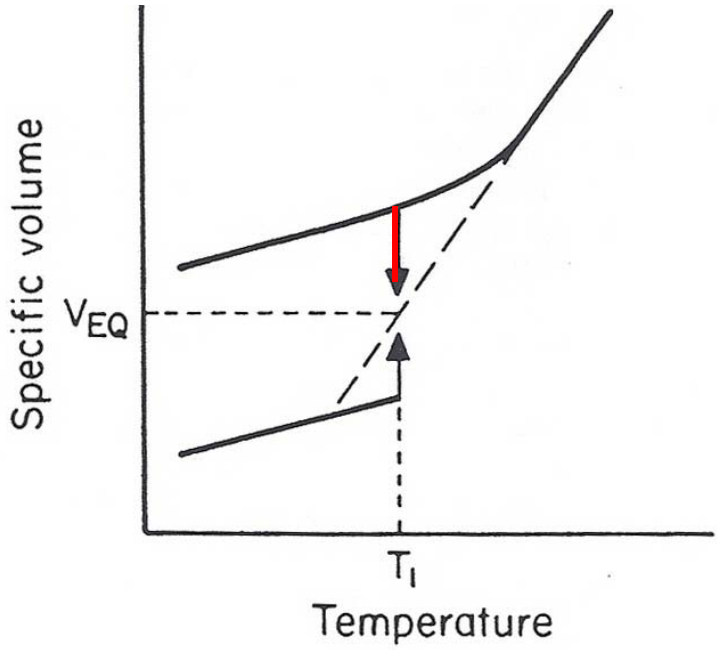

Fig. 9a. Relaxation from initial volumes above and below the equilibrium volume (schematic)

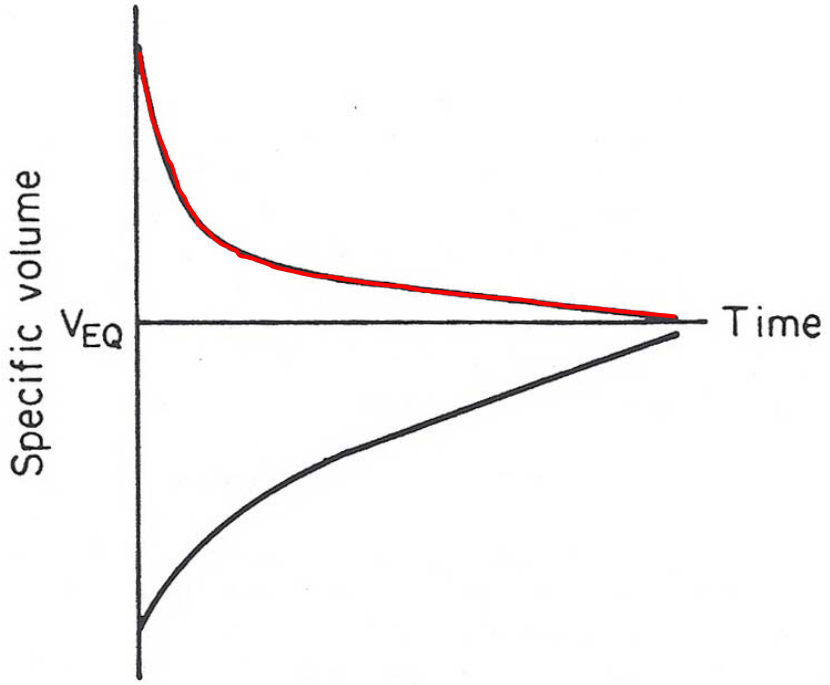

Fig. 9b. Variation of volume with time for initial volumes above and below the equilibrium volume (schematic)

5.7.1 Structural Relaxation

CSRO: Chemical short-range order ⟺ TSRO: Topological short-range order

* Relaxation process

(a) Low temp. regimes (sub-sub-Tg, i.e., Tg-200K <Ta<Tg-100K)

(b) High temp. regimes (sub-Tg, i.e., Ta ≥ Tg-100K)

Exception: Pd-Si, Fe-B and Zr-Cu : undergo structural relaxation just above RT

* Structural relaxation in metallic glasses by a low temperature annealing process

→ does not cause crystallization but significant changes in physical properties

* Relaxed glass : decreased specific heat, reduced diffusivity, reduced magnetic anisotropy, increased elastic constants (by about 7%), significantly increased viscosity (by more than 5 orders of magnitude) and loss of (bend) ductility in some glasses, in addition to changes in elastic resistivity (by about 2 %), Curie temperature (by as much as 40 K), enthalpy (by about 200-300 cal/mol), superconductivity, and several other structure-sensitive properties.

& Density changes: a small increase in density (about 0.5% for melt-spun ribbons and a smaller value of about 0.1%-0.15% for BMG alloys)

5.7.1 Structural Relaxation

* Density changes: a small increase in density (about 0.5% for melt-spun ribbons and a smaller value of about 0.1%-0.15% for BMG alloys)

TABLE 5.3

Changes in the Bulk Densities, ρ (g cm^{-3}) of Metallic Glassy Alloys in the As-Solidified and Structurally Relaxed Conditions

Alloy Composition	Synthesis Method	Rod Diameter (mm)/Ribbon Thickness	$\rho_{as\text{-}solidified}$	$\rho_{relaxed}$	$\Delta\rho_{relaxed}$ (%)	Reference
$Pd_{77.5}Cu_6Si_{16.5}$	Melt spinning	30 μm thick ribbon	10.46	10.51	0.48	[68]
$Pd_{40}Cu_{30}Ni_{10}P_{20}$	Melt spinning	40 μm thick ribbon	9.318	9.337	0.2	[69]
$Pd_{77.5}Cu_6Si_{16.5}$	Water quenching	2 mm dia rod	10.48	10.51	0.29	[68]
$Pd_{40}Cu_{30}Ni_{10}P_{20}$	Cu-mold casting	5 mm dia rod	9.27	9.28	0.11	[70]
$Zr_{55}Cu_{30}Al_{10}Ni_5$	Cu-mold casting	5 mm dia rod	6.82	6.83	0.15	[70]

Note: $$\Delta\rho_{relaxed} = \frac{\rho_{relaxed} - \rho_{as\text{-}solidified}}{\rho_{as\text{-}solidified}}.$$

* Measurement of structural relaxation in metallic glasses:

- Electrical resistivity measurements (CSRO < TSRO) and DSC (most popular technique)
- Mossbauer spectroscopy (determine the atomic environments)
- Hardness measurement (increased)
- Diffraction techniques (X-ray, neutron, and electron scattering methods)

(sharpening of the PDF peaks, without shifting their position)

→ The first stage of relaxation was suggested to be related to the elimination of short and long inter-atomic distances and the second stage to the local chemical reordering in the glassy phase (phase separation and nano-crystallization after annealing at higher temp.

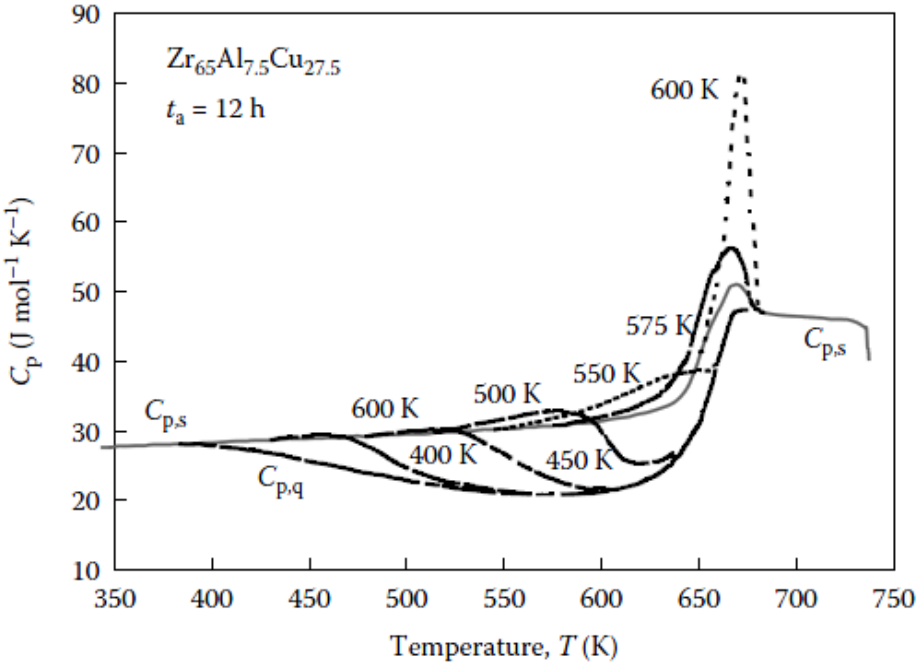

FIGURE 5.12
The variation of specific heat, C_p with annealing temperature, T_a for a glassy $Zr_{65}Al_{7.5}Cu_{27.5}$BMG alloy annealed for 12 h at different temperatures from 400 to 620 K. The solid line represents the variation of C_p for the reference sample annealed for 12 h at 690 K. (Reprinted from Inoue, A. et al., *J. Non-Cryst. Solids*, 150, 396, 1992. With permission.)

→ dependent on thermal history, excess endothermic peak (recoverable), exothermic broad peak (irrecoverable)

* Electrical resistivity measurement during bending fatigue test

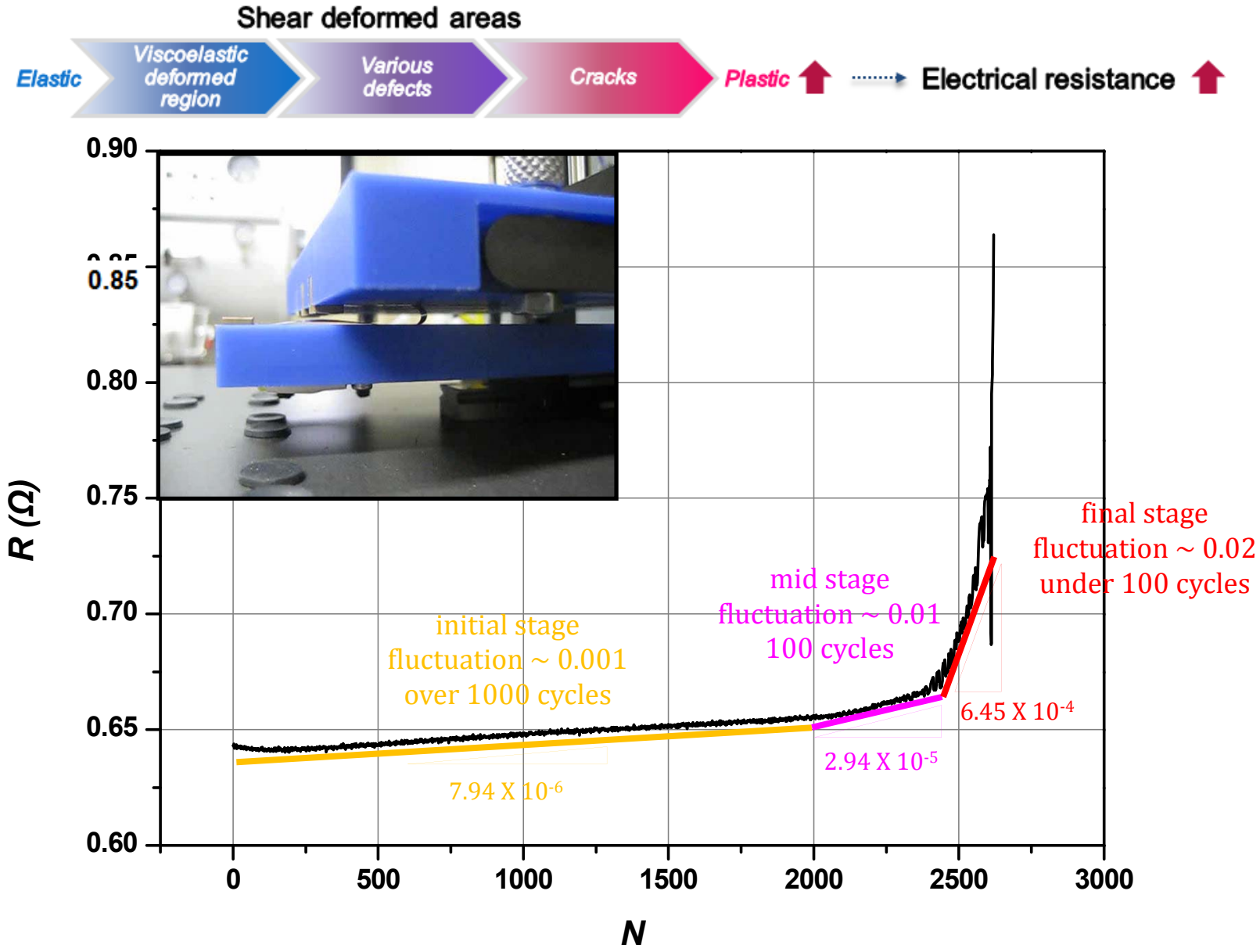

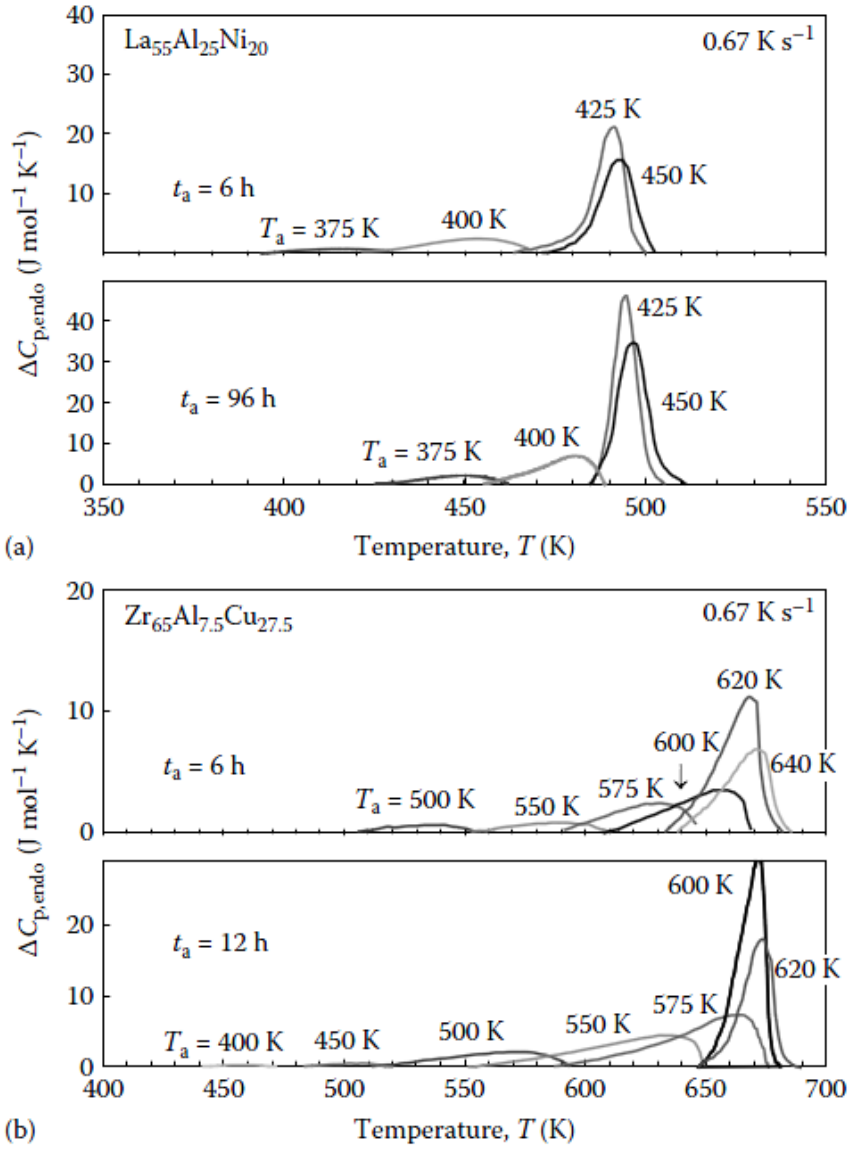

FIGURE 5.13
The differential specific heat, $\Delta C_p(T)$, between the reference and annealed samples for the glassy (a) $La_{55}Al_{25}Ni_{20}$ and (b) $Zr_{65}Al_{7.5}Cu_{27.5}$ alloys annealed for 6 and 96 h for the $La_{55}Al_{25}Ni_{20}$ alloy and for 1 and 12 h in the case of $Zr_{65}Al_{7.5}Cu_{27.5}$ alloy at different temperatures. The samples have been heated in a DSC at 0.67 K s^{-1} (40 K min^{-1}). (Reprinted from Inoue, A. et al., *J. Non-Cryst. Solids*, 150, 396, 1992. With permission.)

* Assuming that the change in enthalpy is entirely due to structural changes in the glassy state and that the average free volume per atom (=V_f/V_m, where V_f is the free volume and V_m is the atomic volume) is proportional to the change in enthalpy:

$$\frac{V_f}{V_m} = C\Delta H \tag{5.5}$$

where C is a constant. The proportionality constant C is determined by first calculating V_f using the Grest and Cohen model [83]:

$$V_f = \frac{k}{2s_0}\left(T - T_0 + \sqrt{(T-T_0)^2 + \frac{4V_a s_0}{k}T}\right) \tag{5.6}$$

$Zr_{44}Ti_{11}Ni_{10}Cu_{10}Be_{25}$ glassy

where k is the Boltzmann constant. The appropriate fit parameters for the above alloy were reported to be: $bV_m s_0/k = 4933\,K$ with $b = 0.105$, $4V_a s_0/k = 162\,K$, $T_0 = 672\,K$. V_m for this alloy has been reported to be 1.67×10^{-29} m^3 near the liquidus temperature. Thus, by calculating V_f from Equation 5.6, V_f/V_m can be calculated.

→ The mechanical properties of metallic glasses (including the BMGs) are affected by the magnitude of free volume present in them. Hence, it becomes important to be able to quantitatively determine the free volume present in the glass to relate the magnitude of free volume to the changes in mechanical properties.

Dynamic mechanical relaxations in typical glasses

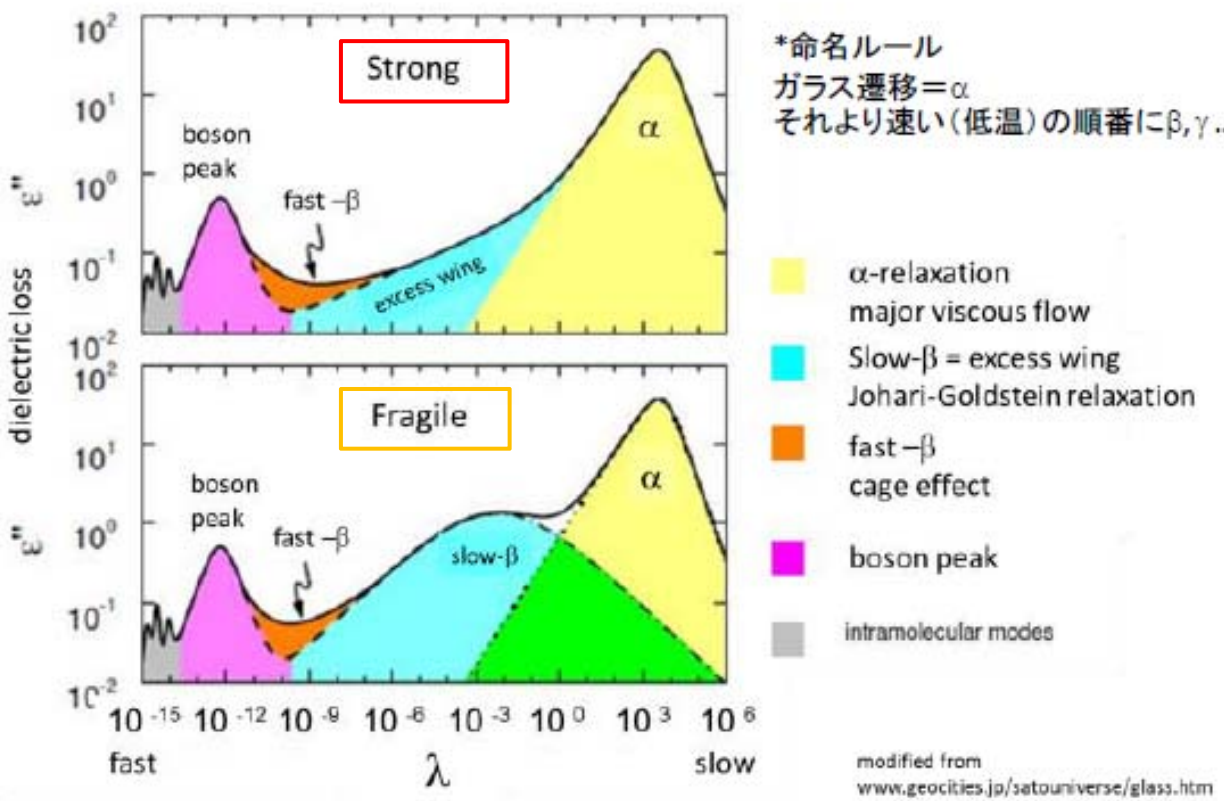

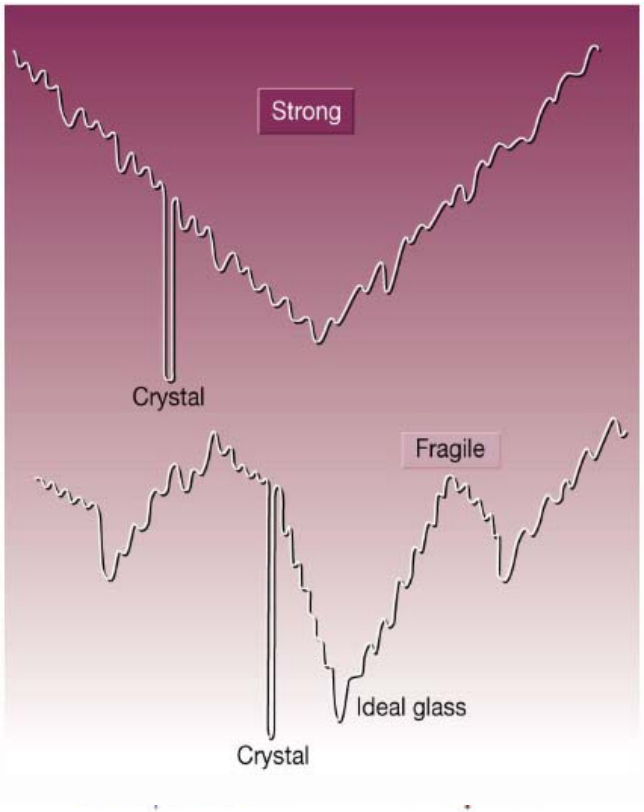

Strong: small deviation of activation E
between α relaxation and β relaxation

Fragile: large deviation of activation E
between α relaxation and β relaxation

Schematic representation of the energy landscapes of strong and fragile substances.

α & β-relaxations observed on the loss modulus in other metallic glasses (La, Pd & Pt based alloys) at ~ their T_g

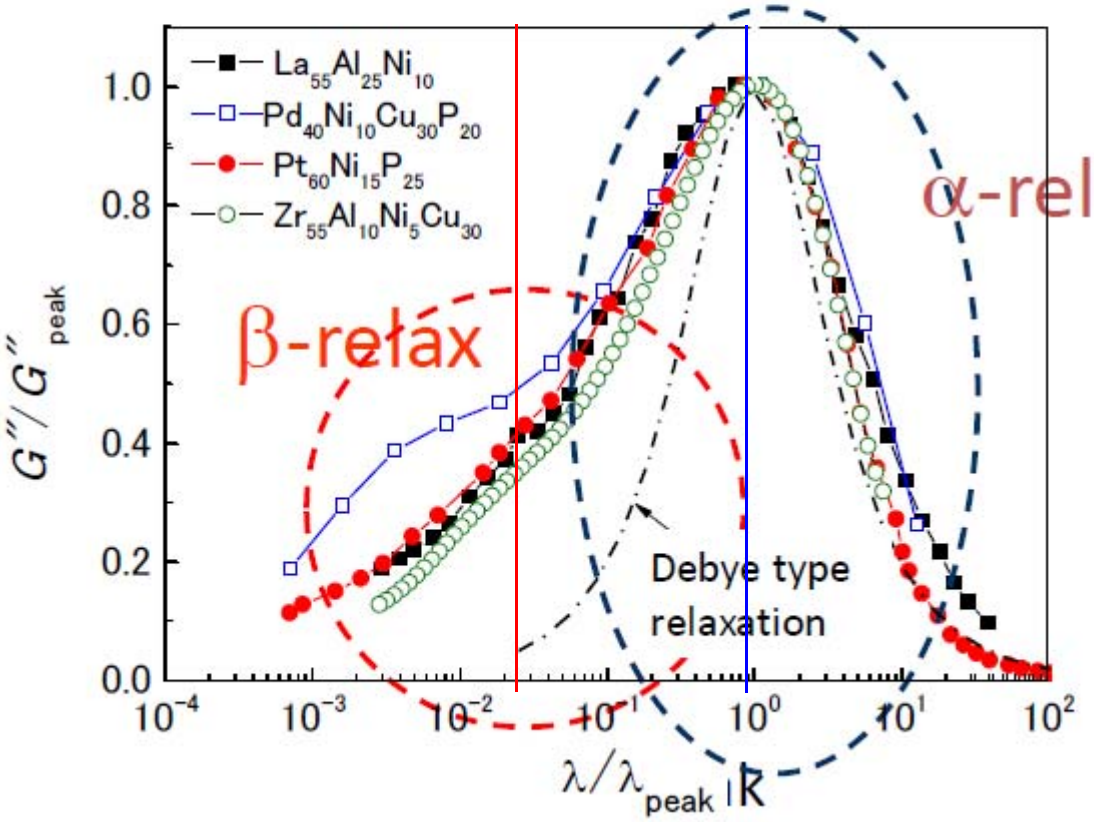

PdNiCuP: α緩和とβ緩和の活性化エネルギー差が大

それ以外: α緩和とβ緩和の活性化エネルギー差が小

Temperature dependence of relaxation time
: α relaxation (VFT) & β relaxation (Arrhenius)

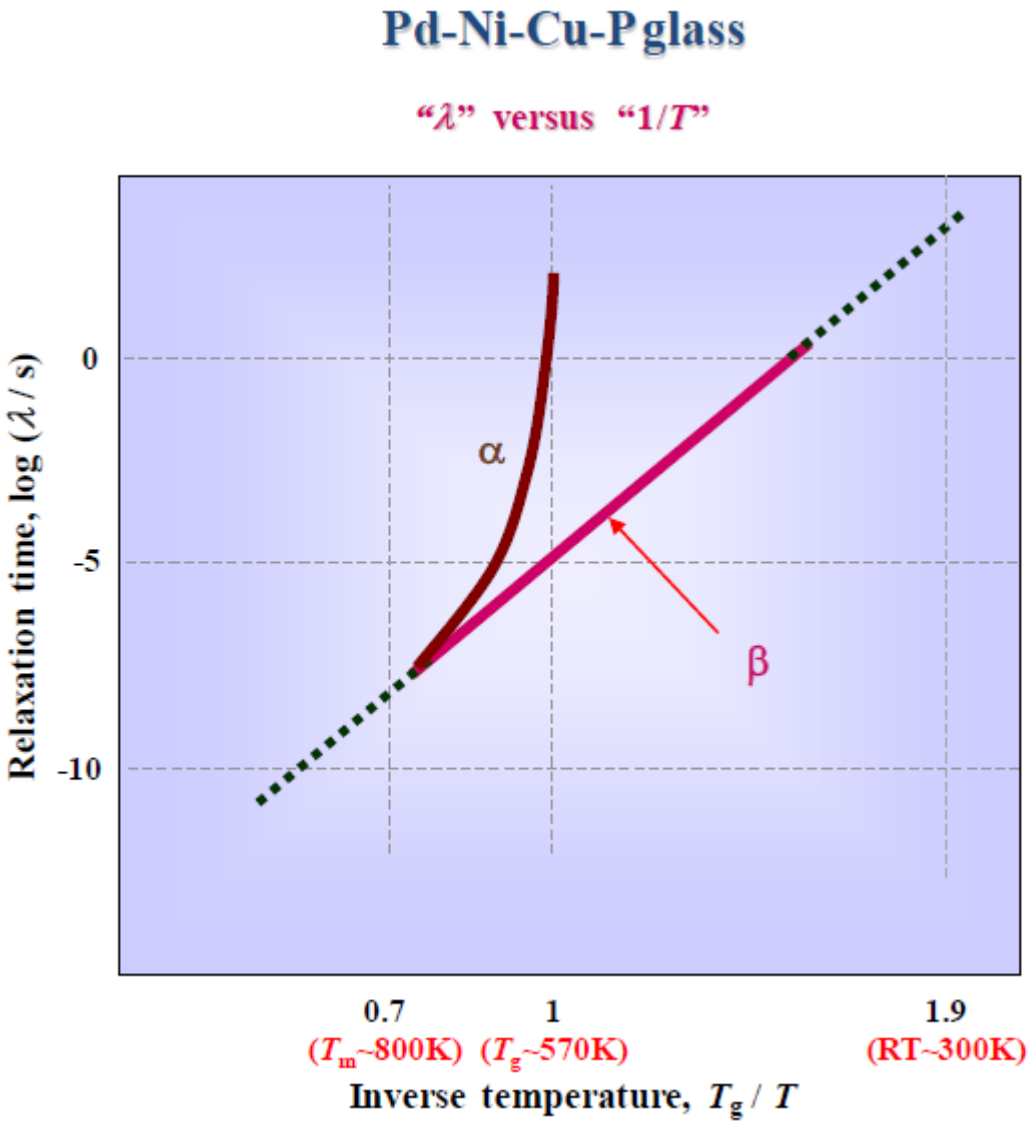

α VFT

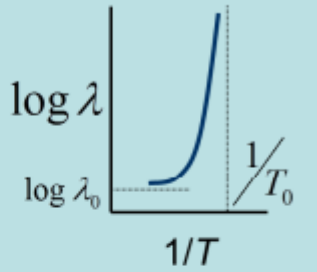

$$\lambda_\alpha = \lambda_{\alpha 0} \exp\left(\frac{Q_\alpha}{T - T_0}\right)$$

Arrhenius β

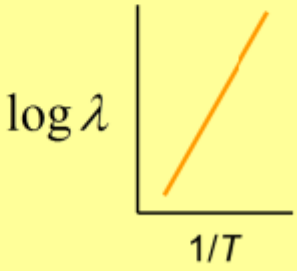

$$\lambda_\beta = \lambda_{\beta,0} \exp\left(\frac{Q_\beta}{kT}\right)$$

緩和が観測されるタイムスケールの温度依存性

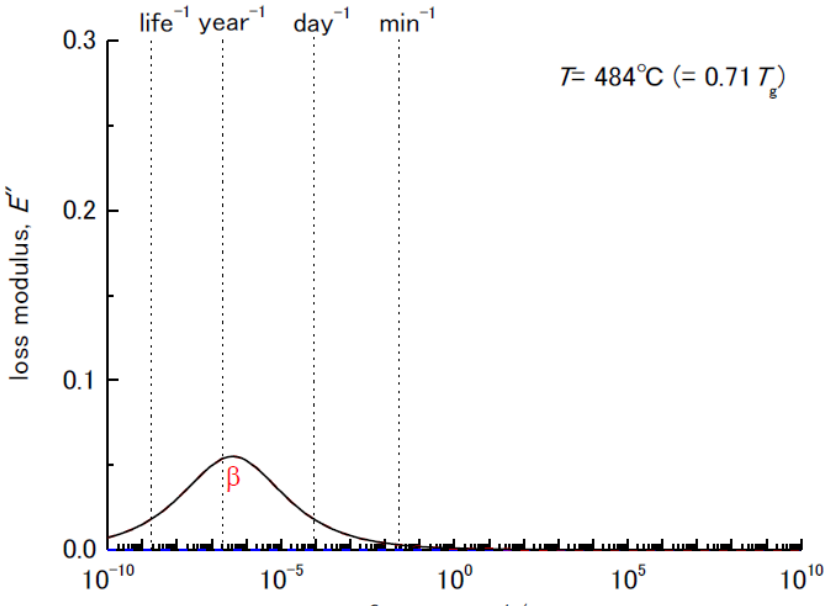

緩和が観測されるタイムスケールの温度依存性

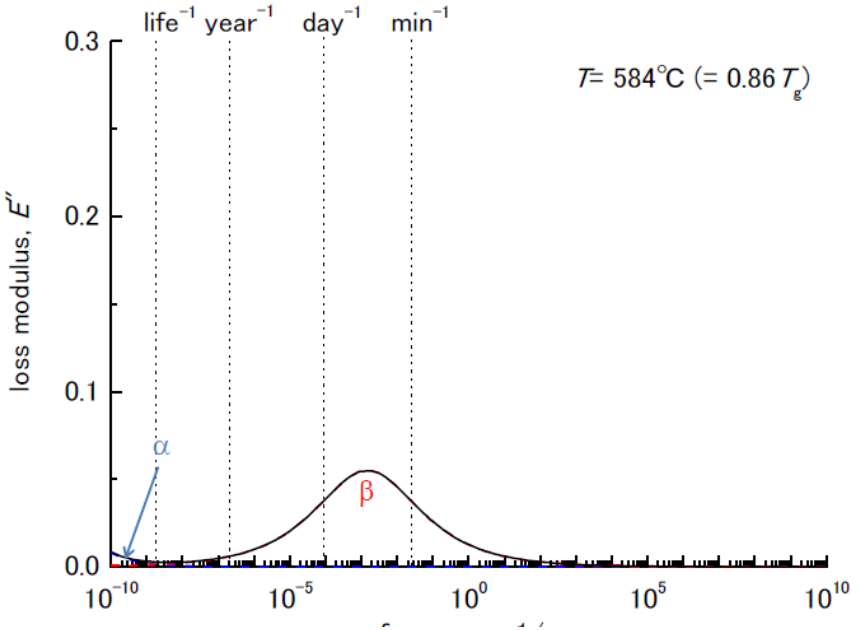

緩和が観測されるタイムスケールの温度依存性

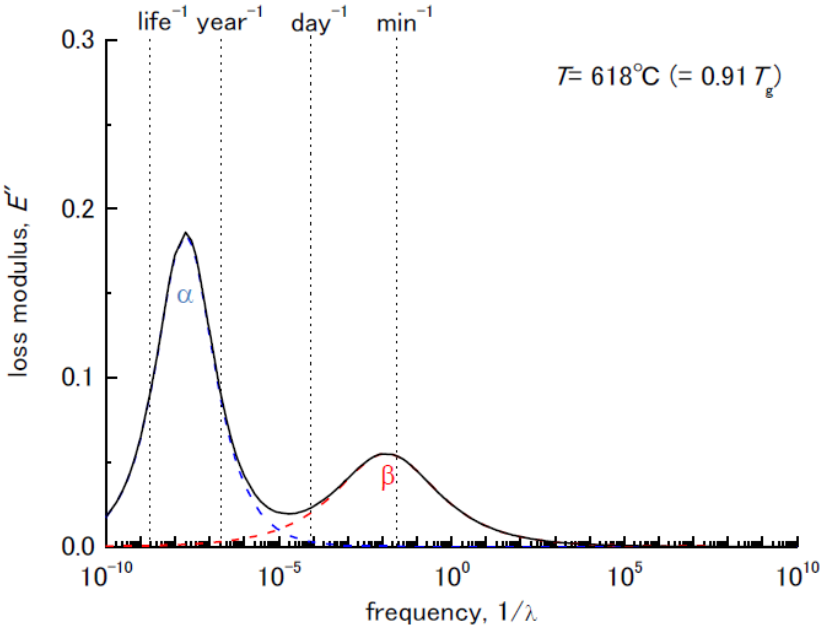

緩和が観測されるタイムスケールの温度依存性

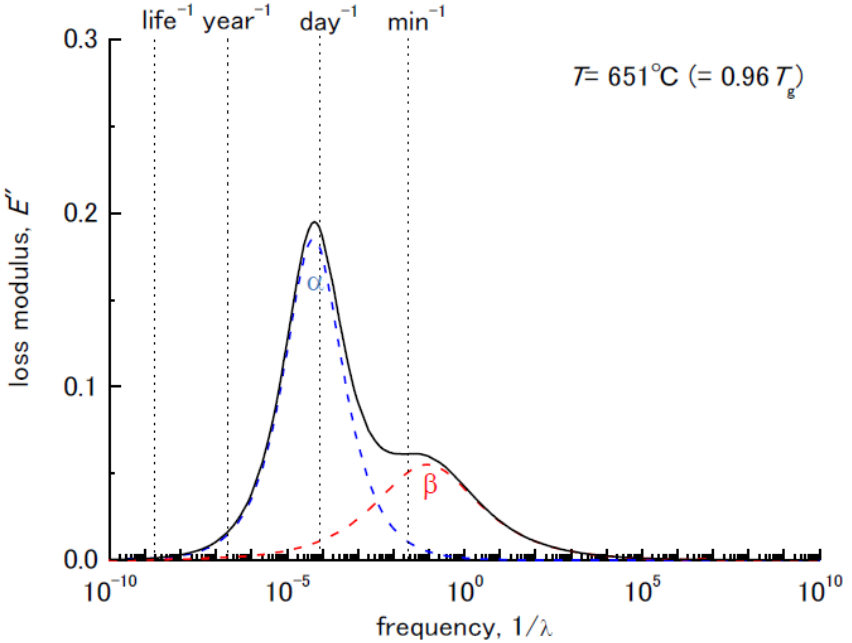

緩和が観測されるタイムスケールの温度依存性

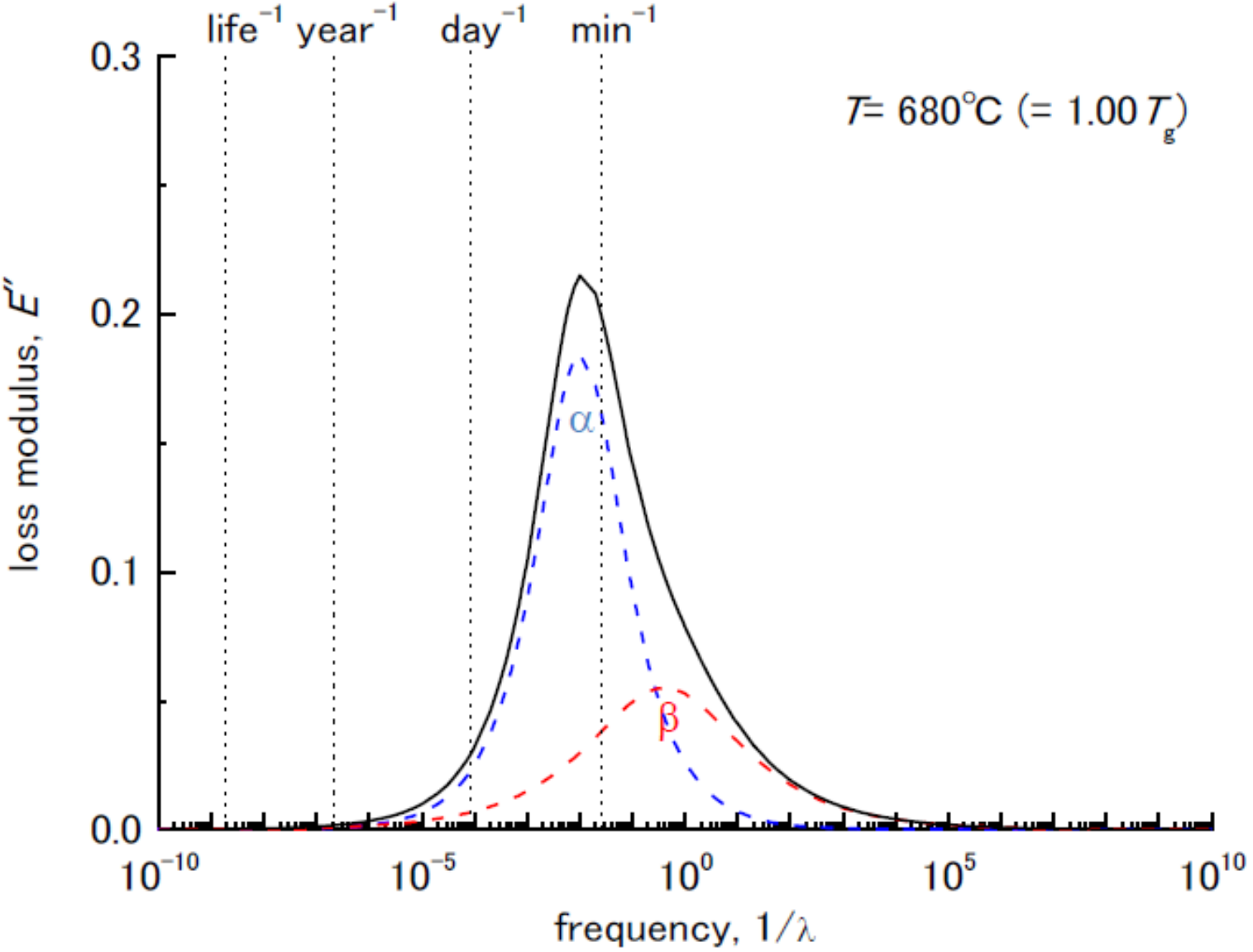

what is the slow-β relaxation, and where it comes from?

Under argument for 40 years

- Homogeneous process

  Williams & Watts, Trans. Faraday Soc. **67**, 1971 (1971).
  Fast, small-angle reorientations of all molecules.
  This motion is restricted to smaller amplitudes than the primary process.

- Inhomogeneous process "Islands of mobility"

  Johari & Goldstein, J. Phys. Chem. **53**, 2372 (1970).
  In regions of lower density "islands of mobility" molecules can partially reorient, giving rise to the process.

  ➢ **Johari-Goldstein relaxation**

Which is true for metallic glass?

structural inhomogeneity correlating to slow-β

- Weakly & strongly bonded regions

  Ichitsubo et al, PRL95, 245501 (2005)
  & JNCS357, 494 (2011)

  The size ξ of SBR
  ~ 4 nm in Pd-Ni-Cu-P
  ~1.5 nm in Zr-Al-Ni-Cu

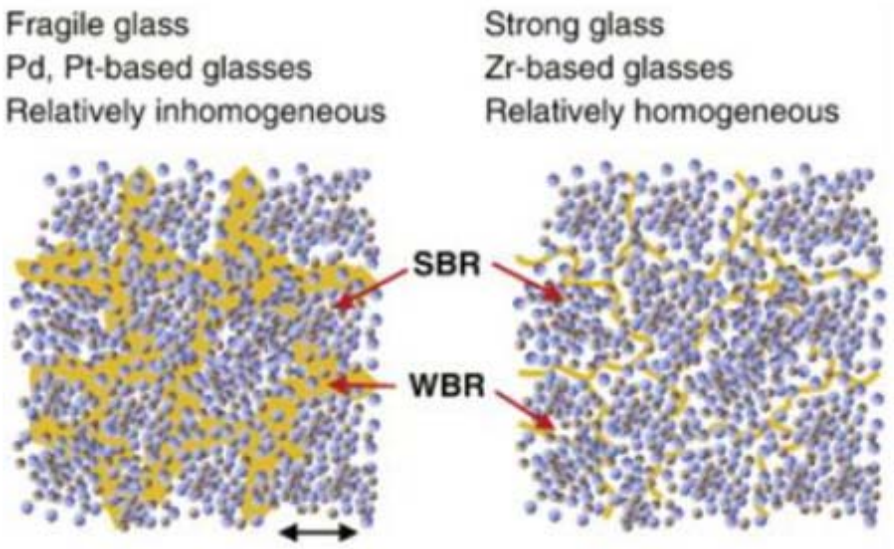

WBR, JG-relaxation & STZ

Wang et al, PRB75, 174201 (2007)
Local motion in the loser region below Tg
Q_β~ 28.4*RTg* (alloy dependence)

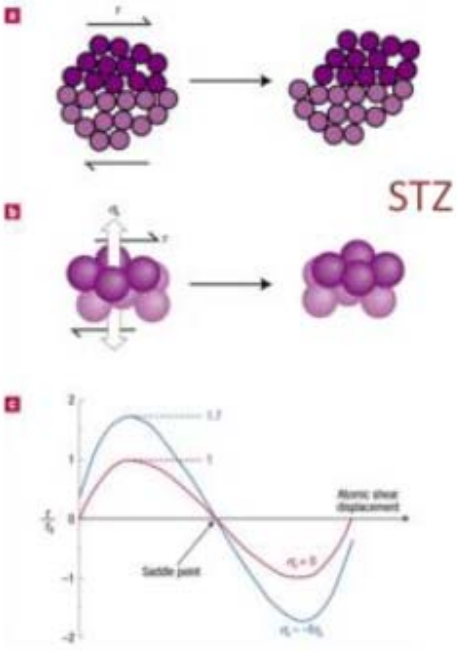

Wang et al, PRB81, 220201(R) (2010)
Slow β site ~ Shear Transformation Zone
by showing direct correlation between W_{STZ}~E_β.

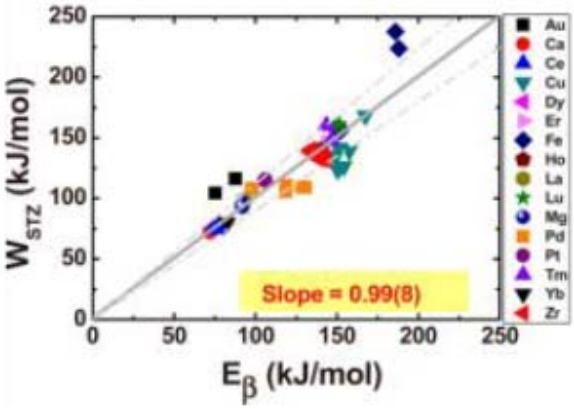

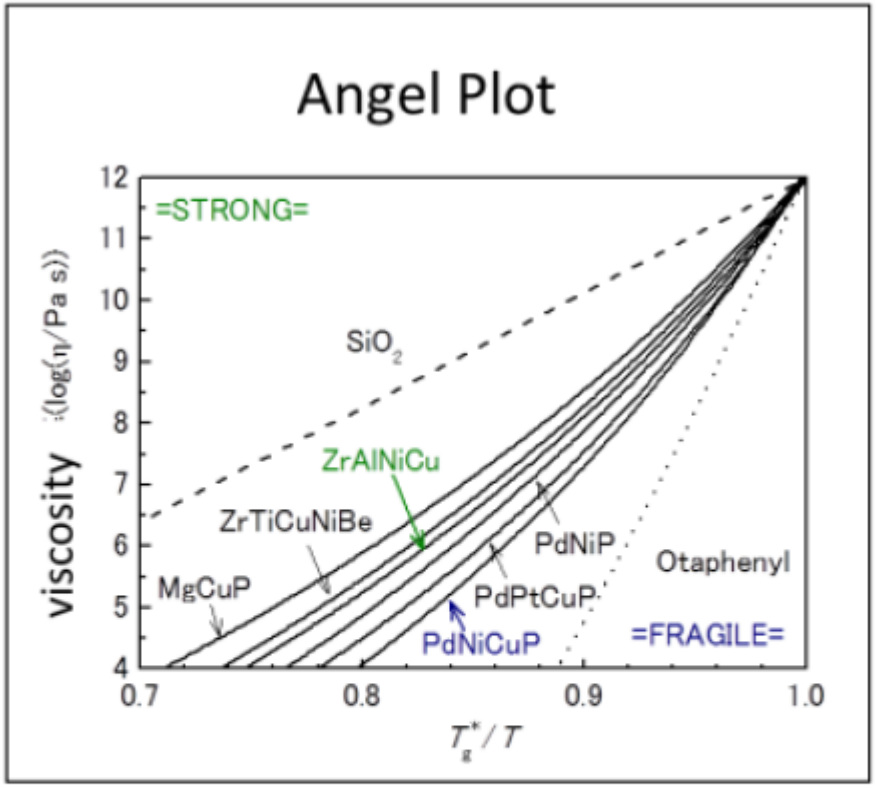

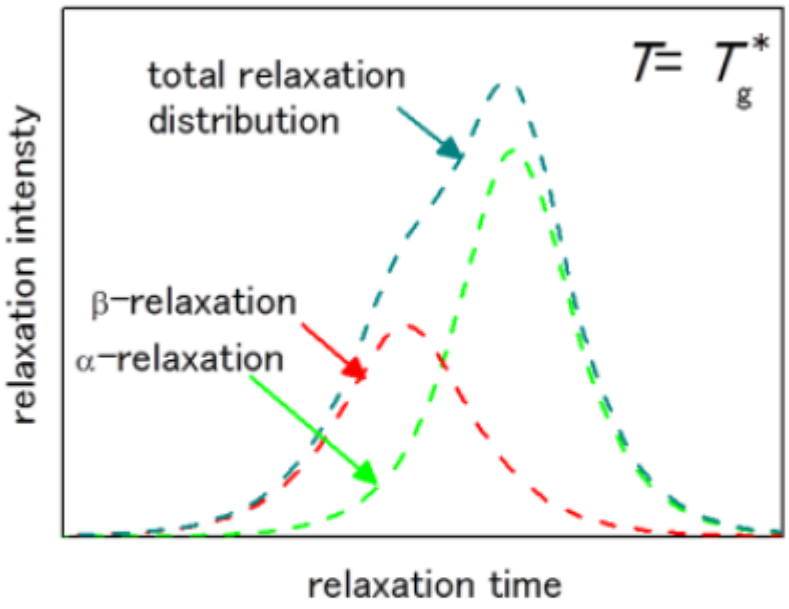

dominating as the same with plasticity, toughness at RT

viscosity and its temperature dependence is determined by the correlation between α- & β-relaxations.

5.7.2 Glass Transition: abrupt variation of C_p

Acta Materialia 59 (2011)

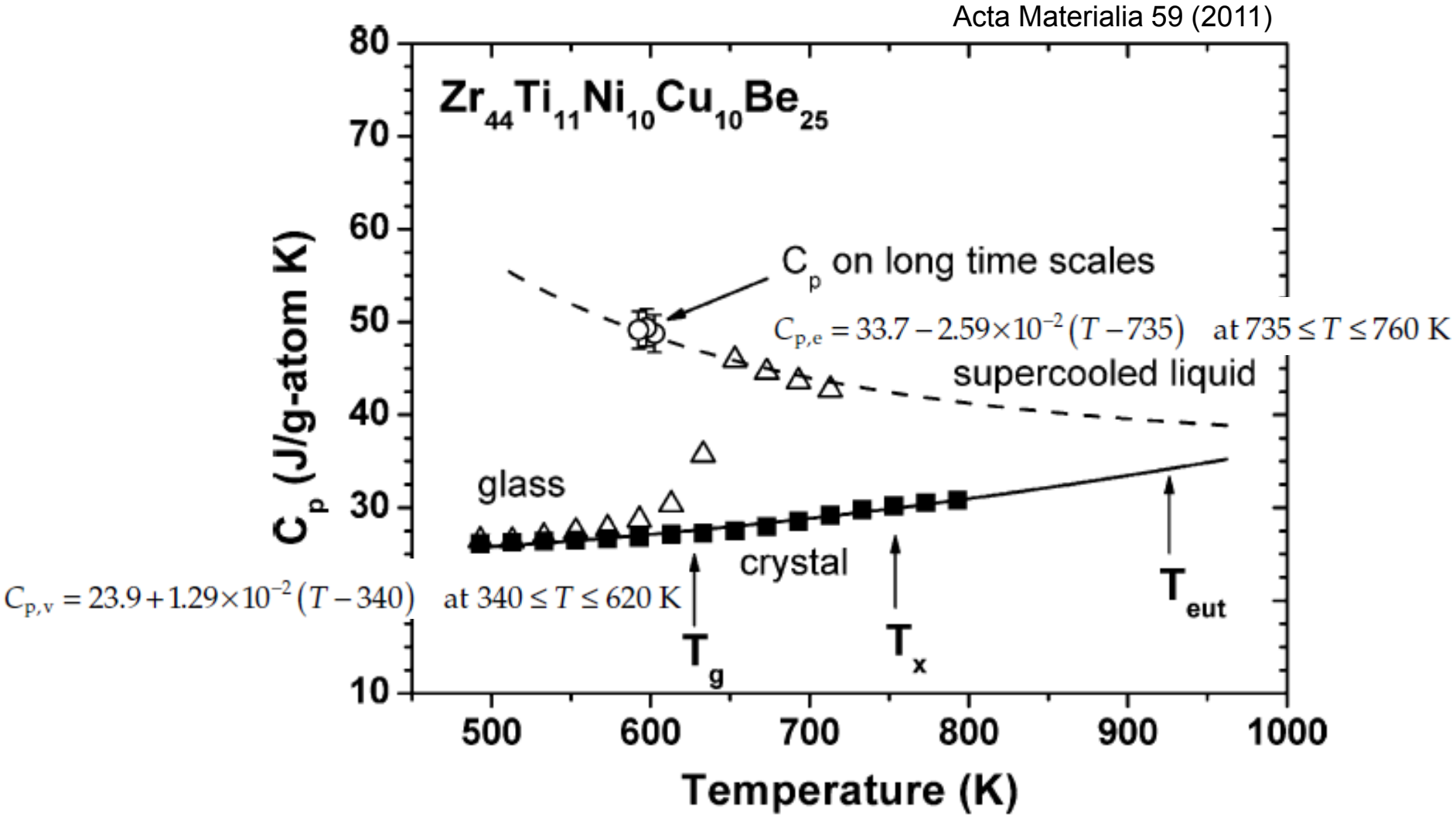

- **Ideal glass transition temperature (T_{oc} =T_g^0)**

: lower temperature limit to occur glass transition thermodynamically

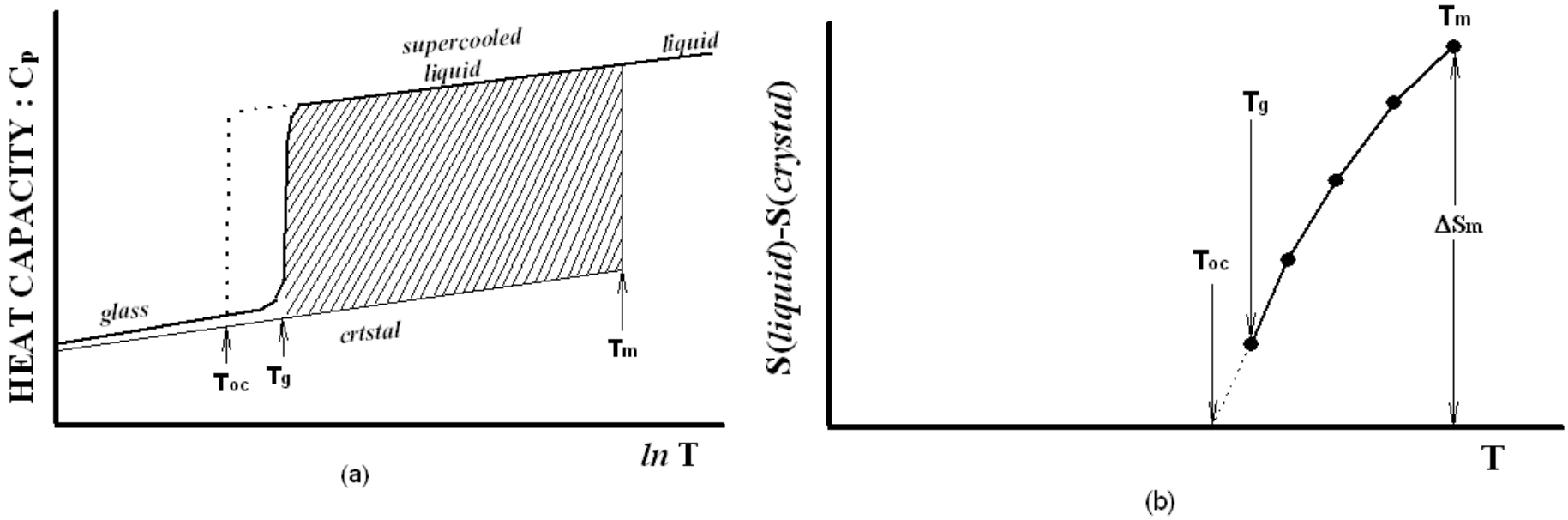

Variation of (a) C_p and (b) excess entropy, S depending on temp. for glass, crystal and liquid. Ideal glass transition temp, T_{oc}. is the temperature when excess entropy is disappeared.

TABLE 5.4

Increase in Specific Heat from the As-Quenched Glassy (g) State to the Supercooled Liquid (scl) Condition, $\Delta C_{p,g\rightarrow scl}$ for Different Metallic Glasses Synthesized by Melt Spinning, and Measured at a Heating Rate of 0.67 K s^{-1} (40 K min^{-1})

Composition	$\Delta C_{p,g\rightarrow scl}$ (J mol^{-1} K^{-1})	ΔT_x (K)	Reference
$La_{55}Al_{20}Cu_{25}$	11.5	59	[84]
$La_{55}Al_{25}Ni_{20}$	14.0	69	[85]
$Mg_{50}Ni_{30}La_{20}$	17.4	58	[86]
$Zr_{60}Al_{15}Ni_{25}$	6.25	77	[87]
$Zr_{65}Cu_{27.5}Al_{7.5}$	—	88	[75]
$Zr_{65}Cu_{17.5}Ni_{10}Al_{7.5}$	14.5	127	[15]

Note: ΔT_x represents the width of the supercooled liquid region.

The $\Delta C_{p,g\rightarrow scl}$ values for the Zr-based metallic glasses are considerably smaller than those of Pd–Ni–P and Pt–Ni–P glasses. Even though the reasons for this difference are not clearly known at the moment, it is possible that it is related to (1) the higher packing fraction of atoms in the glassy Zr-alloys, which require a lower cooling rate to form the glassy structure, (2) the possibility of the atomic configuration in the glassy and supercooled liquid structures being similar, and (3) the higher T_g values in comparison to those of La-, Mg-, Pd-, and Pt-based glassy alloys.

Overshoot in heating process

When the kinetics become fast enough to allow the sample to regain metastable equilibrium

Determined from DSC up-scan

$$\int_{T^*}^{T_f'} (C_p^e - C_p^g) dT_f = \int_{T^*}^{T'} (C_p - C_p^g) dT$$

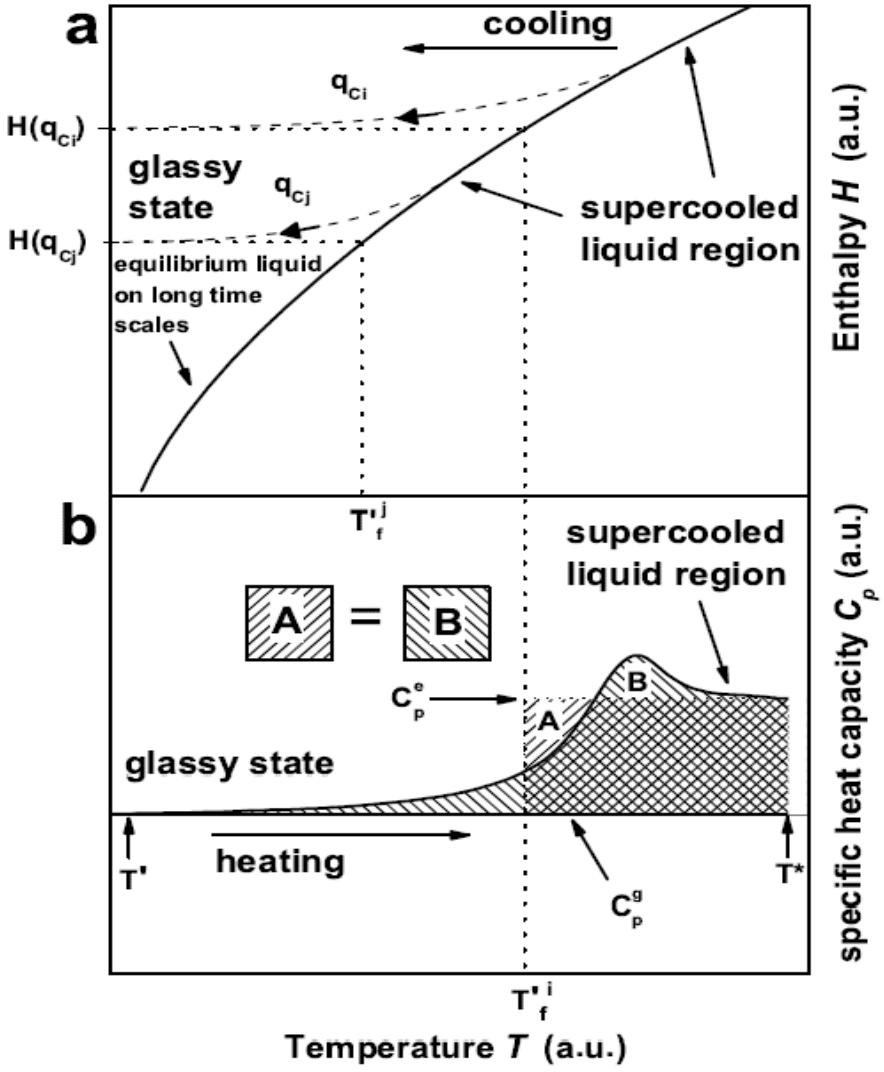

J. Appl. Phys. 107, 123529 (2010)

5.7.3 Phase separation

2-Amorphous phases

Polymer

(AFM)
PGMA/PS

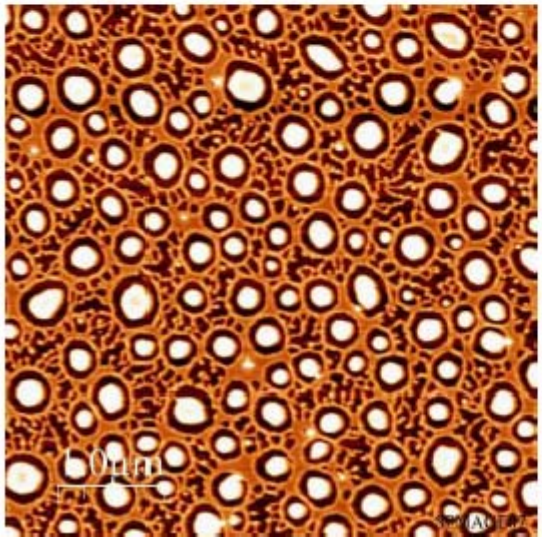

Oxide glass

(SEM)
SiO_2-NaO_2

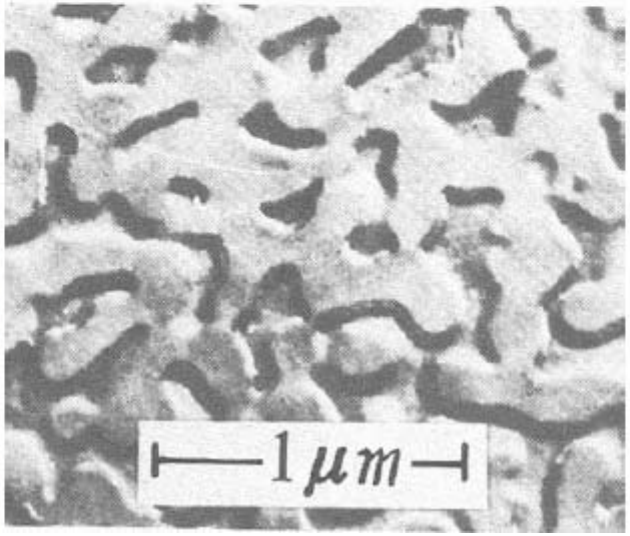

Metallic glass

(TEM)
TiYAlCo

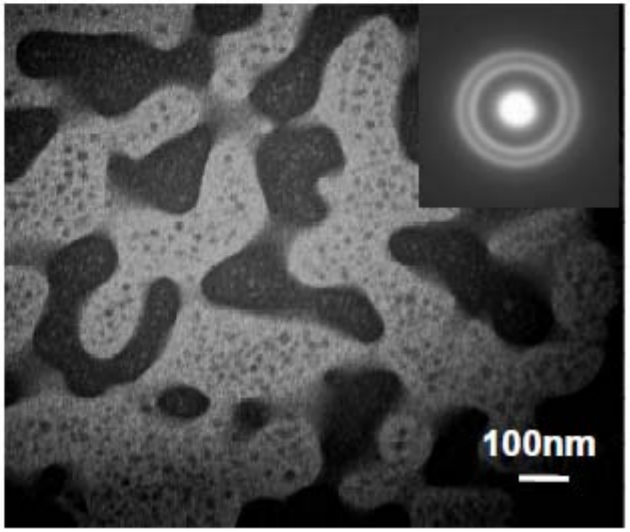

* Miscibility gaps in phase separating system

- **Stable immiscibility**

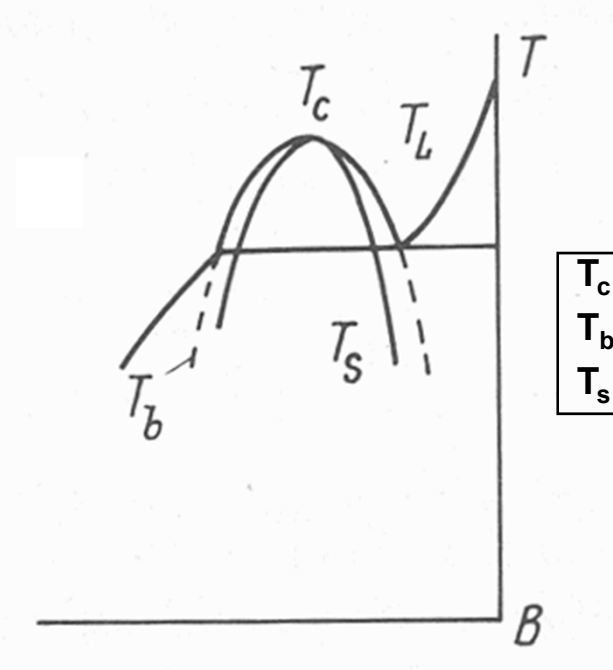

T_c : critical temperature
T_b : binodal curve
T_s : spinodal curve

immiscibility above the liquidus

⇒ decomposition into stable liquid

- **Metastable immiscibility**

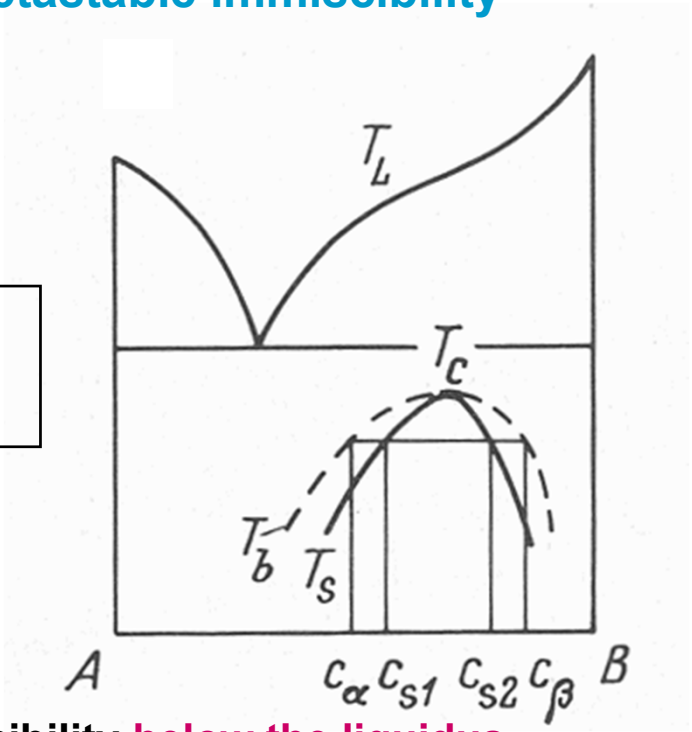

immiscibility below the liquidus

⇒ decomposition into metastable liquid

"Phase separation in glass" ed. by Mazurin and Porai-Koshits (1984)

(a) Positive heat of mixing relation among constituent elements

- **Alloy design considering heat of mixing relation among constituent elements**

$\Delta H_{mix} \gg 0$ between A & B

⬇

creates (meta)stable miscibility gap in limited composition range

⬇

Phase separation to A-rich & B-rich phase

- **Different two-phase structure by initial composition before phase separation**

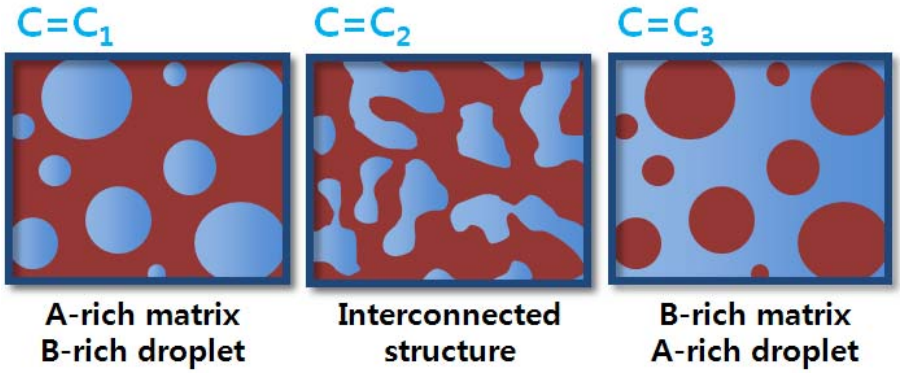

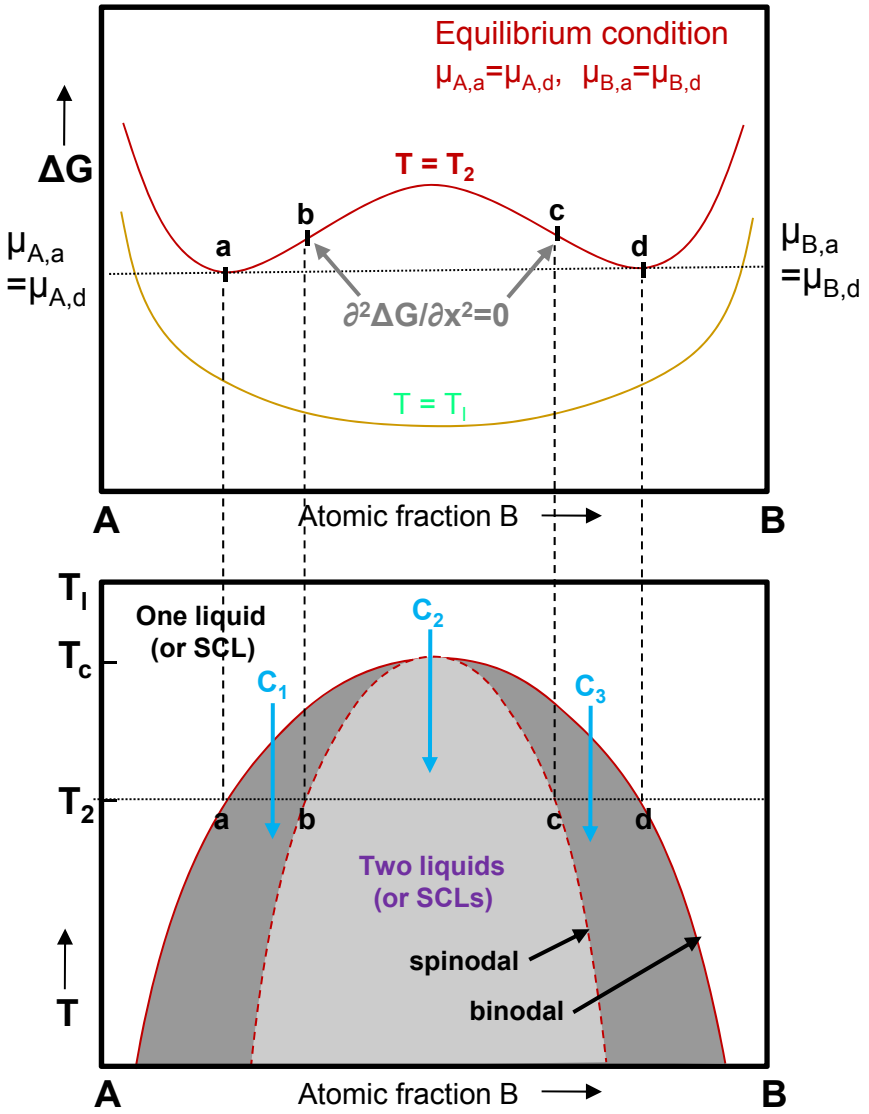

Nucleation and growth ↔ Spinodal decomposition without any barrier to the nucleation process

3D image construction process - $Gd_{30}Ti_{25}Al_{25}Co_{20}$

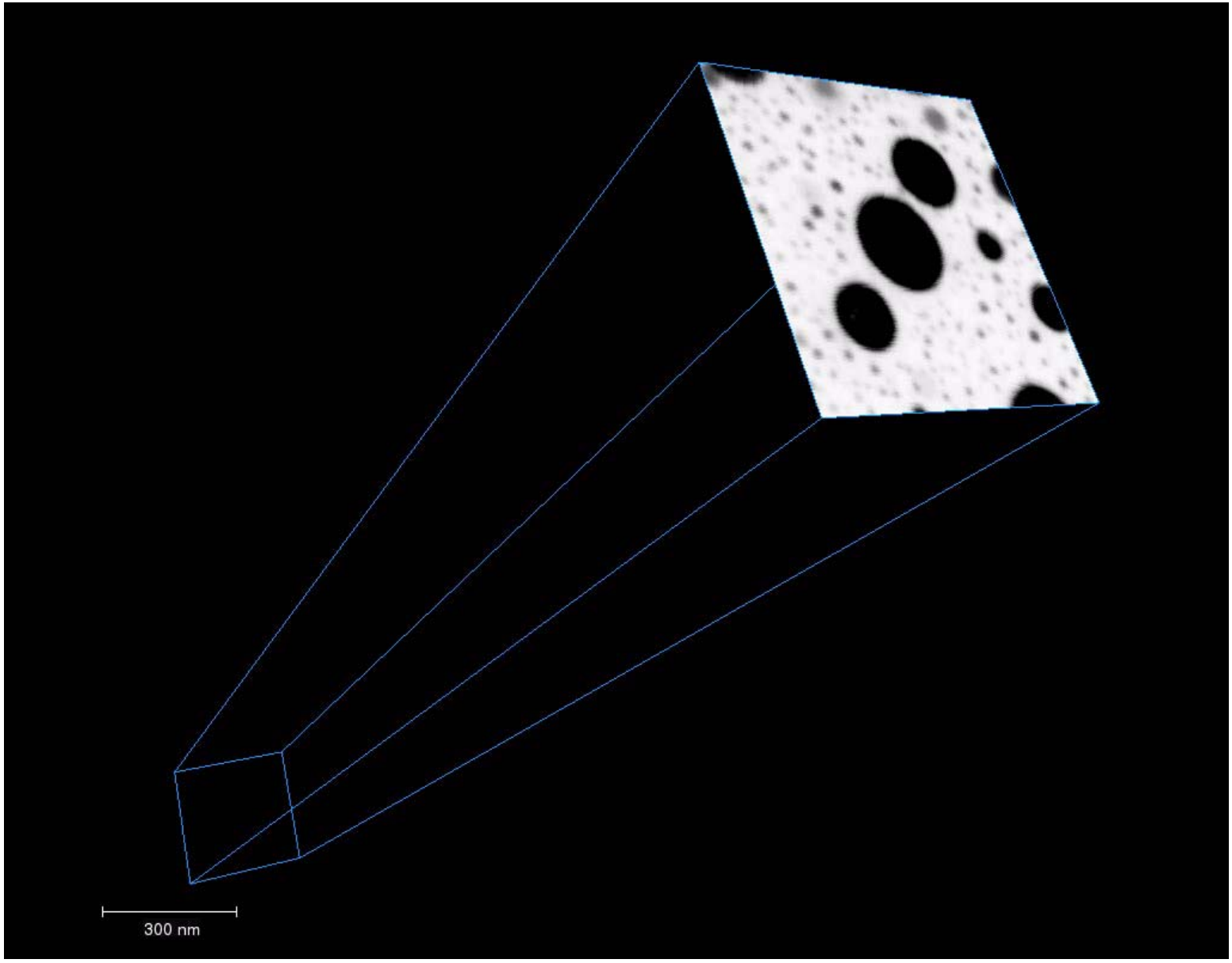

3D microstructure of phase separated metallic glass

Wheel side

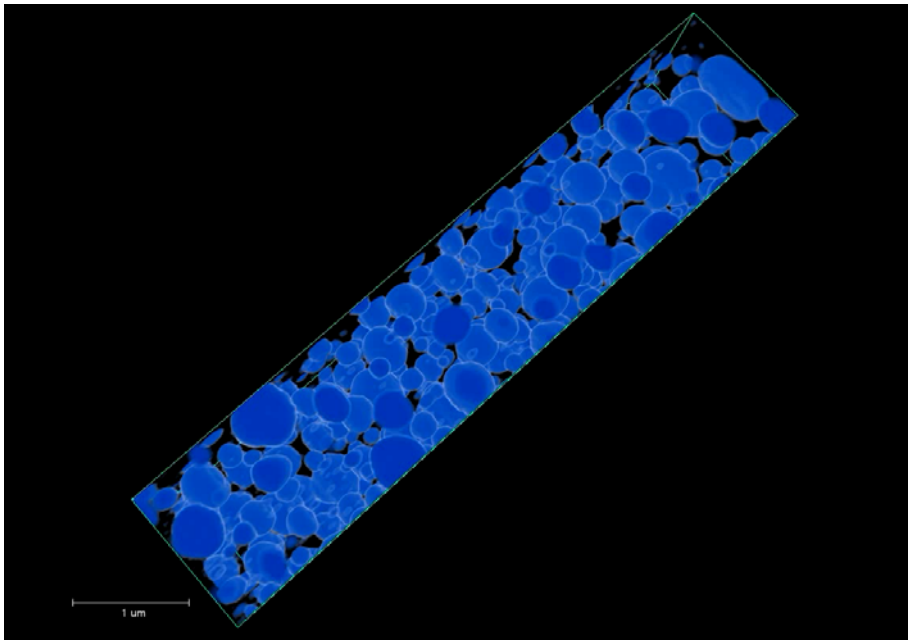

Free side

Volume fraction = 33.78%

Wheel side

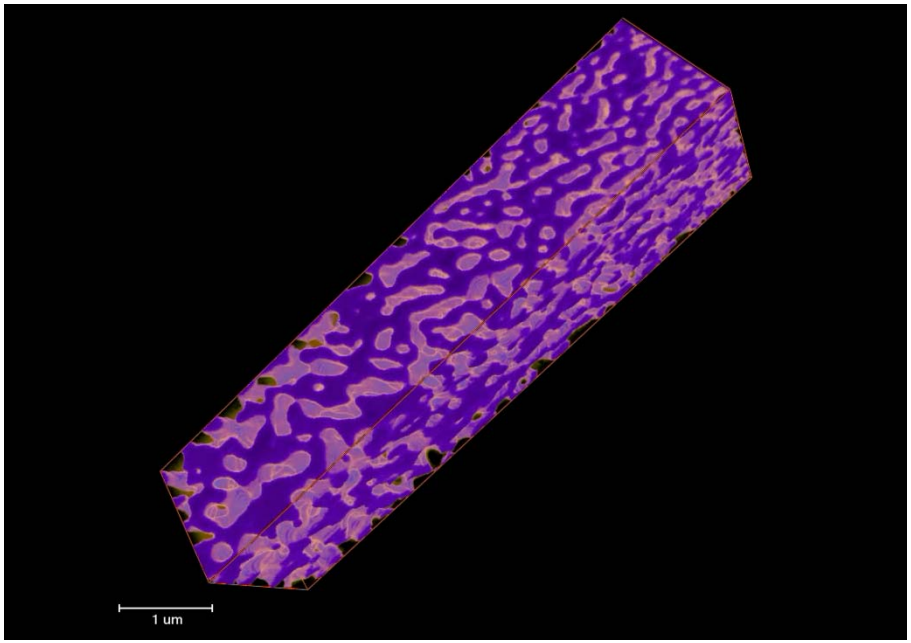

Free side

Volume fraction = 48.74%

It is possible to tailor the sizes of the glassy phases by varying the solidification rate during cooling.